Importance of Correlation Effects on Magnetic Anisotropy in Fe and Ni

Imseok Yang, Sergej Y. Savrasov, and Gabriel Kotliar

Department of Physics and Astronomy and Center for Condensed Matter Theory, Rutgers University, Piscataway, NJ 08854

(February 1, 2008)

We calculate magnetic anisotropy energy of Fe and Ni by taking into account the effects of strong electronic correlations, spin-orbit coupling, and non-collinearity of intra-atomic magnetization. The LDA+U method is used and its equivalence to dynamical mean–field theory in the static limit is emphasized. Both experimental magnitude of MAE and direction of magnetization are predicted correctly near $U = 4\ eV$ for Ni and $U = 3.5\ eV$ for Fe. Correlations modify one–electron spectra which are now in better agreement with experiments.

PACS numbers: 71.15.Mb 71.15.Rf 71.27.+a 75.30.Gw 75.40.Mg

The calculation of the magneto-crystalline anisotropy energy (MAE) [1–5] of magnetic materials containing transition-metal elements from first principles electronic structure calculations is a long-standing problem. The MAE is defined as the difference of total energies with the orientations of magnetization pointing in different, e.g., (001) and (111), crystalline axis. The difference is not zero because of spin-orbit effect, which couples the magnetization to the lattice, and determines the direction of magnetization, called the easy axis.

Being a ground state property, the MAE should be accessible in principle via density functional theory (DFT) [6,7]. Despite the primary difficulty related to the smallness of MAE ($\sim 1\ \mu eV$/atom), great efforts to compute the quantity with advanced total energy methods based on local density approximation (LDA) combined with the development of faster computers, have seen success in predicting its correct orders of magnitudes [8–12]. However, the correct easy axis of Ni has not been predicted by this method and the fundamental problem of understanding MAE is still open.

A great amount of work has been done to understand what is the difficulty in predicting the correct axis for Ni. Parameters within the LDA calculation have been varied to capture physical effects which might not be correctly described. These include (i) scaling spin-orbit coupling in order to enlarge its effect on the MAE [9,10], (ii) calculating torque to avoid comparing large numbers of energy [10], (iii) studying the effects of the second Hunds rule in the orbital polarization theory [11], (iv) analyzing possible changes in the position of the Fermi level by changing the number of valence electrons [12], (v) using the state tracking method [13], and (iv) real space approach [14].

In this paper we take a new view that the correlation effects within the d shell are important for the magnetic anisotropy of $3d$ transition metals like Ni. These effects are not captured by the LDA but are described by Hubbard–like interactions presented in these systems and need to be treated by first principles methods [15].

Another effect which has not been investigated in the context of magnetic anisotropy calculations is the non-collinear nature of intra-atomic magnetization [16]. It is expected to be important when spin-orbit coupling and correlation effects come into play together. In this article we show that when we include these new ingredients into the calculation we solve the long-standing problem of predicting the correct easy axis of Ni.

We believe that the physics of transition metal compounds is intermediate between atomic limit where the localized d electrons are treated in the real space and fully itinerant limit when the electrons are described by band theory in k space. A many–body method incorporating these two important limits is the dynamical mean–field theory (DMFT) [17]. The DMFT approach has been extensively used to study model Hamiltonian of correlated electron systems in the weak, strong and intermediate coupling regimes. It has been very successful in describing the physics of realistic systems, like the transition metal oxides and, therefore, is expected to treat properly the materials with d or f electrons.

Electron-electron correlation matrix $U_{\gamma_1\gamma_2\gamma_3\gamma_4} = \langle m_1 m_3 | v_C | m_2 m_4 \rangle \delta_{s_1 s_2} \delta_{s_3 s_4}$ for d orbitals is the quantity which takes strong correlations into account. This matrix can be expressed via Slater integrals $F^{(i)}$, $i = 0, 2, 4, 6$ in the standard manner. The inclusion of this interaction generates self–energy $\Sigma_{\gamma_1\gamma_2}(i\omega_n, \vec{k})$ on top of the one–electron spectra. Within DMFT it is approximated by momentum independent self–energy $\Sigma_{\gamma_1\gamma_2}(i\omega_n)$.

A central quantity of the dynamical mean–field theory is the one–electron on–site Green function

$$G_{\gamma_1\gamma_2}(i\omega_n) = \sum_{\vec{k}} \left[(i\omega_n + \mu)O_{\gamma_1\gamma_2}(\vec{k}) - H^0_{\gamma_1\gamma_2}(\vec{k}) \right.$$
$$\left. + \ v_{dc} - \Sigma_{\gamma_1\gamma_2}(i\omega_n) \right]^{-1}. \qquad (1)$$

where $H^0_{\gamma_1\gamma_2}(\vec{k})$ is the one-electron Hamiltonian standardly treatable within the LDA. Since the latter already includes the electron-electron interactions in some averaged way, we subtract the double counting term v_{dc} [18]. The use of realistic localized orbital representation such as linear muffin–tin orbitals [19] leads us to include overlap matrix $O_{\gamma_1\gamma_2}(\vec{k})$ into the calculation.

The DMFT reduces the problem to solving effective impurity model where the correlated d orbitals are treated as an impurity level hybridized with the bath of conduction electrons. The role of hybridization is played by the so–called bath Green function defined as follows:

$$[\mathcal{G}_0^{-1}]_{\gamma_1\gamma_2}(i\omega_n) = G_{\gamma_1\gamma_2}{}^{-1}(i\omega_n) + \Sigma_{\gamma_1\gamma_2}(i\omega_n). \qquad (2)$$

Solving this impurity model gives access to the self–energy $\Sigma_{\gamma_1\gamma_2}(i\omega_n)$ for the correlated electrons. The one–electron Green function (1) is now modified with new $\Sigma_{\gamma_1\gamma_2}(i\omega_n)$, which generates a new bath Green function. Therefore, the whole problem requires self–consistency.

In this paper we confine ourselves to zero temperature and make an additional assumption on solving the impurity model using the Hartree–Fock approximation. In this approximation the self–energy reduces to

$$\Sigma_{\gamma_1\gamma_2} = \sum_{\gamma_3\gamma_4}(U_{\gamma_1\gamma_2\gamma_3\gamma_4} - U_{\gamma_1\gamma_2\gamma_4\gamma_3})\bar{n}_{\gamma_3\gamma_4} \qquad (3)$$

where $\bar{n}_{\gamma_1\gamma_2}$ is the average occupation matrix for the correlated orbitals. The off-diagonal elements of the occupancy matrix are not zero when spin-orbit coupling is included [20]. The latter can be implemented following the prescription of Andersen [19] or more recent one by Pederson [21].

In the Hartree–Fock limit the self–energy is frequency independent and real. The self–consistency condition of DMFT can be expressed in terms of the average occupation matrix: Having started from some $\bar{n}_{\gamma_1\gamma_2}$ we find $\Sigma_{\gamma_1\gamma_2}$ according to (3). Fortunately, the computation of the on–site Green function (1) needs *not* to be performed. Since the self–energy is real, the new occupancies can be calculated from the eigenvectors of the one–electron Hamiltonians with $\Sigma_{\gamma_1\gamma_2} - v_{dc}$ added to its dd block. The latter can be viewed as an orbital–dependent potential which has been introduced by the LDA+U method [15].

The LDA+U method has been very successful compared with experiments at zero temperature in ordered compounds. By establishing its equivalence to the static limit of the DMFT we see clearly that dynamical mean–field theory is a way of improving upon it, which is crucial for finite temperature properties.

In this work we study the effect of the Slater parameter F_0 that is the Hubbard on site interaction U on the magnetic anisotropy energy. The latter is calculated by taking the difference of two total energies with different directions of magnetization (MAE=$E(111) - E(001)$). The total energies are obtained via fully self consistent solutions. Since the total energy calculation requires high precision, full potential LMTO method [22] has been employed. For the $\vec{k}$ space integration, we follow the analysis given by Trygg and co–workers [11] and use the special point method [23] with a Gaussian broadening [24] of 15 mRy. The validity of this procedure has been tested in their work [11]. For convergence of the total energies within desired accuracy, about 15000 k-points are needed. We used 28000 k-points to reduce possible numerical noise. Our calculations include non-spherical terms of the charge density and potential both within the atomic spheres and in the interstitial region [22]. All low-lying semi-core states are treated together with the valence states in a common Hamiltonian matrix in order to avoid unnecessary uncertainties. These calculations are spin polarized and assume the existence of long-range magnetic order. Spin-orbit coupling is implemented according to the suggestions by Andersen [19]. We also treat magnetization as a general vector field, which realizes non-collinear intra-atomic nature of this quantity. Such general magnetization scheme has been recently discussed in [16].

We now discuss our calculated MAE. We first test our method in case of LDA ($U = 0$). To compare with previous calculations, we turn off the non-collinearity of magnetization which makes it collinear with the quantization axis. The calculation gives correct orders of magnitude for both fcc Ni and bcc Fe but with the wrong easy axis for Ni, which is the same result as the previous result [11]. Turning on the non-collinearity results in a a larger value of the absolute value of the MAE (2.9 μeV) for Ni but the easy axis predicted to be (001) which is still wrong. The magnitude of the experimental MAE of Ni is 2.8 μeV aligned along (111) direction [25].

We now describe the effect of strong correlations, which is crucial in predicting the correct axis of Ni (see Fig. 1). As U increases, the MAE of Ni smoothly increases until U reaches 2.5 eV and then smoothly decreases up to the value 3.8 μeV. Around $U = 3.9$ eV, the MAE decreases abruptly to negative value. Around $U = 4.0$ eV, the experimental order of magnitude and the correct easy axis (111) are restored. The change from the wrong easy axis to the correct easy axis occurs over the range of $\delta U \sim 0.2 eV$, which is the order of spin-orbit coupling constant ($\sim 0.1 eV$).

For Fe, the MAE decreases on increasing U to negative values, where the magnetization takes the wrong axis. From $U = 2.7$ eV, it increases back to the correct direction of easy axis (positive MAE). Around $U = 3.5$ eV, it restores the correct easy axis and the experimental value of MAE is reproduced.

It is remarkable that the values of U necessary to reproduce the correct magnetic anisotropy energy are very close to the values which are needed to describe photoemission spectra of these materials [26]. This shows an internal consistency of our approach and emphasizes the importance of correlations.

We find direct correlation between the dependency of the MAE as a function of U and the difference of magnetic moments ($\Delta M = -(M(111) - M(001))$) behaving similarly. For Ni, the difference of magnetic moments is nearly U independent up to $U = 3$ eV. For large U, it smoothly decreases from the positive value to the negative one. It also decreases rapidly around $U = 3.9$ eV in accord with MAE. For Fe, the difference is positive at $U = 0$. It decreases slightly to the negative values and then increases to the positive value over the range of $U < 2.7$ eV where MAE decreases. For larger U's, where MAE is coming back to positive value, its slope is significantly larger than that at smaller U's.

This concurrent change of MAE and the difference of magnetic moments suggests why some previous attempts

based on force theorem [12] failed in predicting the correct easy axes. Force theorem replaces the difference of the total energies by the difference of one–electron energies. In this approach, the contribution from the slight difference in magnetic moments does not appear and, therefore, is not counted in properly. Unfortunately, we could not find any experimental data of magnetic moments to the desired precision $(10^{-4}\mu_B)$ to compare with. We also have problems in reaching the convergence of the total energy with desired accuracy for large values of U in both Fe and Ni.

We now present implications of our results on the calculated electronic structure for the case of Ni. One important feature which emerges from the calculation is the absence of the X_2 pocket (see Fig. 2). This has been predicted by LDA but has not been found experimentally [27]. The band corresponding to the pocket is pushed down well below the Fermi level. This is expected since correlation effects are more important for slower electrons and the velocity near the pocket is rather small. It turns out that the whole band is submerged under the Fermi level.

There has been some suspicions that the incorrect position of the X_2 band within LDA was responsible for the incorrect prediction of the easy axis within this theory. Daalderop and coworkers [12] removed the X_2 pocket by increasing the number of valence electrons and found the correct easy axis. We therefore conclude that the absence of the pocket is one of the central elements in determining the magnetic anisotropy, and there is no need for any ad-hoc adjustment within a theory which takes into account the correlations.

We now describe the effects originated from (near) degenerate states close to the Fermi surface. These have been of primary interest in past analytic studies [28,29]. We will call such states *degenerate Fermi surface crossing* (DFSC) states. The contribution to MAE by non-DFSC states comes from the fourth order perturbation. Hence it is of the order of λ^4. The energy splitting between DFSC states due to spin-orbit coupling is of the order of λ because the contribution comes from the first order perturbation. Using linear approximation of the dispersion relation $\epsilon(\vec{k}\lambda)$, the relevant volume in k-space was found of the order λ^3. Thus, these DFSC states make contribution of the order of λ^4. However, there may be accidentally DFSC states appearing along a line on the Fermi surface, rather than at a point. We have found this case in our LDA calculation for Ni. Therefore the contribution of DFSC states is as important as the bulk non-DFSC states though the degeneracies occur only in small portion of the Brillouin zone.

The importance of the DFSC states leads us to comparative analysis of the LDA and LDA+U band structures near the Fermi level. In LDA, five bands are crossing the Fermi level at nearly the same points along the ΓX direction. Two of the five bands are degenerate for the residual symmetry and the other three bands accidentally cross the Fermi surface at nearly the same points. There are two sp bands with spin up and spin down, respectively. The other three bands are dominated by d orbitals. In LDA+U, one of the d bands is pushed down below the Fermi surface. The other four bands are divided into two degenerate pieces at the Fermi level (see Fig. 2): Two symmetry related degenerate $d_\downarrow$ bands and two near degenerate $sp_\uparrow$ and $sp_\downarrow$ bands. In LDA, we found that two bands are accidentally near degenerate along the line on the Fermi surface within the plane $\Gamma X L$. One band is dominated by $d_\downarrow$ orbitals. The other is dominated by $s_\downarrow$ orbitals near X and by $d_\downarrow$ orbitals off X. In LDA+U, these accidental DFSC states disappear(see Fig. 2). Instead, there is new two-fold DFSC states along ΓL direction, both of which are dominated by $d_\downarrow$ orbitals.

As we have seen, the on-site repulsion U reduces the number of DFSC states along ΓX direction while increasing that of DFSC states along ΓL direction. Based on the tight–binding model, Mori and coworkers [29] have shown that DFSC states along ΓL direction result in the magnetization aligned along $(1, 1, 1)$ direction and DFSC states along ΓX direction result in the magnetization aligned along $(0, 0, 1)$ direction. Since the strong correlation does precisely this, we conclude that disappearance of DFSC states along ΓX direction and their appearance along ΓL direction is another important element that determines the easy axis of Ni.

Unlike LDA, we have found two extra very tiny L pockets in LDA+U (see Fig. 2). Both of them are dominated by sp orbital with opposite spins. Being small, these extra pockets may be artifacts of LDA+U.

To conclude, we have demonstrated that it is possible to perform highly precise calculation of the total energy in order to obtain both the correct easy axes and the magnitudes of MAE for Fe and Ni. This has been accomplished by including the strong correlation effect via the Hubbard-like on-site repulsion U and incorporating the non–collinear magnetization. In both Fe and Ni, the on-site U takes physically acceptable values consistent with the values known from atomic physics. The calculations performed are state of the art in what can currently be achieved for realistic treatments of correlated solids. Further studies should be devoted to improving the quality of the solution of the impurity model within DMFT and extending the calculation to finite temperatures.

[1] J. H. van Vleck, Phys. Rev. **52**, 1178 (1937).

[2] H. Brooks, Phys. Rev. **58**, 909 (1940).

[3] G. C. Fletcher, Proc. R. Soc. London **67A**, 505 (1954).

[4] J. C. Sloncewskij, J. Phys. Soc. Jpn. **17**, Suppl. B (1962).

[5] M. Asdente and M. Delitala, Phys. Rev. **163**, 497 (1967).

[6] P. Hohenberg and W. Kohn, Phys. Rev. **136**, 864 (1964).

[7] W. Kohn and L. J. Sham, Phys. Rev. **140**, 1133 (1965).

[8] H. Eckardt, L. Fritsche, and J. Noffke, J. Phys. F **17**, 943 (1987).

[9] S. V. Halilov *et al.*, Phys. Rev. B **57**, 9557 (1998).

[10] H. J. F. Jansen, J. Appl. Phys. **67**, 4555 (1990).

[11] J. Trygg, B. Johansson, O. Eriksson, and J. M. Willis, Phys. Rev. Lett. **75**, 2871 (1995).

[12] G. H. O. Daalderop, P. J. Kelly, and M. F. H. Schuurmans, Phys. Rev. B **41**, 11 919 (1990).

[13] D. Wang, R. Wu, and A. J. Freeman, Phys. Rev. Lett. **70**, 867 (1993).

[14] S. V. Beiden, W. M. Temmerman, Z. Szotek, G. A. Gehring, G. M. Stocks, Y. Wang, D. M. C Nicholson, W. A. Shelton, and H. Ebert, Phys. Rev. B **57**, 14 247, (1998).

[15] For a review, see, e.g., *Strong Correlations in electronic structure calculations*, edited by V. I. Anisimov (Gordon and Breach Science Publishers, Amsterdam, 2000).

[16] L. Nordstrom and D. Singh, Phys. Rev. Lett. **76**, 4420 (1996).

[17] A. Georges, G. Kotliar, W. Krauth, and M. Rozenberg, Rev. Mod. Phys. **68**, 13 (1996).

[18] A. I. Liechtenstein, V. I. Anisimov, and J. Zaanen, Phys. Rev. B **12**, 3060 (1975).

[19] O. K. Andersen, Phys. Rev. B **12**, 3060 (1975).

[20] I. Y. Solovyev, A. I. Liechtenstein, and K. Terakura, Phys. Rev. Lett. **80**, 5758 (1999).

[21] M. R. Pederson and S. N. Khanna, Phys. Rev. B **60**, 9566 (1999).

[22] S. Y. Savrasov, Phys. Rev. B **54**, 16470 (1996).

[23] S. Froyen, Phys. Rev. B **39**, 3168 (1989). A. P. Cracknell, J. Phys. C **2**, 1425 (1969).

[24] R. J. Needs, R. M. Martin, and O. H. Nielsen, Phys. Rev. B **33**, 3778 (1986). K.-M. Ho, C. L. Fu, and B. N. Harmon, Phys. Rev. Lett. **49**, 673 (1982).

[25] M. B. Stearns, in *Magnetic Properties of 3d, 4d, and 5d Elements, Alloys and Compounds*, Vol. III of *Landolt-Börnstein, New Series*, edited by K.-H. Hellewege and O. Madelung, (Springer-Verlag, Berlin, 1987).

[26] M. Katsenelson and A. Lichtenstein, J. Phys. Cond. Matt. **11**, 1037 (1999). M. Katsenelson and A. Lichtenstein, Phys. Rev. B **61**, 8906 (2000).

[27] C. S. Wang and J. Callaway, Phys. Rev. B **9**, 4897 (1973). F. Weling and J. Callaway, Phys. Rev. B **26**, 710 (1982).

[28] E. I. Kondorskii and E. Straube, Sov. Phys.-JETP **36**, 188 (1973).

[29] N. Mori, Y. Fukuda, and T. Ukai, J. Phys. Soc. Jpn. **37**, 1263 (1974).
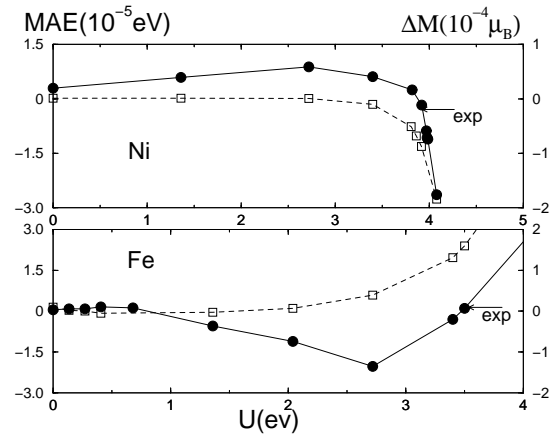
FIG. 1. Experimental and calculated magnetocrystalline anisotropy energy MAE $= E(111) - E(001)$ (filled circle) and the difference of magnetic moment $\Delta M = M(001) - M(111)$ (square) for Fe (top) and Ni(bottom). Experimental MAEs are marked by arrows for Fe (1.4 μeV) and Ni (-2.8 μeV).
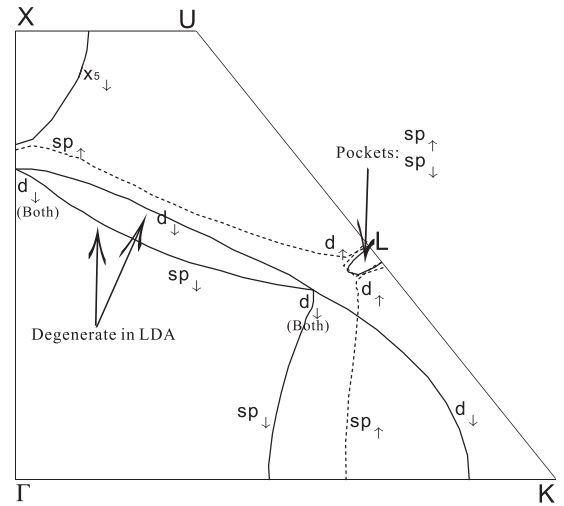

FIG. 2. Calculated Fermi Surface of Ni with the correlation effects taken into account. The solid and dotted lines correspond to majority and minority dominant spin carriers. Dominant orbital characters are expressed. Both experimentally confirmed X_5 pocket and L neck can be seen. The X_2 pocket is missing, which is in agreement with experiments. There are two small L pockets, which has not been found by experiments.